Nonlinear plasmonic frequency conversion through quasiphase matching

Zi-jian Wu, Xi-kui Hu, Zi-yan Yu, Wei Hu, Fei Xu,*,† and Yan-qing Lu*,‡
College of Engineering and Applied Sciences and National Laboratory of Solid State Microstructures, Nanjing University, Nanjing 210093, China

(Received 9 September 2010; published 6 October 2010)

An efficient frequency conversion scheme of surface-plasmon polariton (SPP) is proposed for nonlinear plasmonic applications. Lossy coupling wave equations are deduced to describe the interaction among involved SPP frequency components. The reciprocal vector of a microstructure could partially compensate the SPP wave-vector mismatch through quasiphase matching (QPM). As an example, the frequency doubling of SPP over a periodically poled lithium niobate is studied. The high-field concentration of SPP greatly enhanced the second-harmonic generation (SHG) over a short traveling distance. Although the high attenuation of SPP affects the SHG severely, a long-range SPP SHG is further proposed and investigated, which shows great efficiency improvement. The applications of QPM SPP frequency conversion are also discussed showing great potentials in miniature plasmonic sources and processors.

DOI: 10.1103/PhysRevB.82.155107 PACS number(s): 73.20.Mf, 42.65.Ky, 78.20.Bh

I. INTRODUCTION

Plasmonics is a recently emerged exciting technology in photonics community, which exploits the unique properties of surface-plasmon polariton (SPP) to enable routing of light at the nanoscale.[1,2] In contrast to conventional dielectric waveguides, SPP simultaneously carries optical and electrical signals, which gives rise to new capabilities in future optical interconnects. Further progress thus requires the development of radically new technologies that can facilitate signal transport and manipulation in nanomicron-to-submicron scale at optical frequencies. Up to date, SPP refraction,[3] reflection,[4] interference,[5] and far-field detection[6] have been realized. Even SPP photonic crystal has been demonstrated.[7] On the other hand, nonlinear optics has been a proven tool to process signals in light domain, such as all-optical switching[8,9] and single photon detection.[10,11] Quasiphase-matched (QPM) materials are good examples among them,[8,12–14] in which periodically poled $LiNbO_3$ (PPLN) is a typical representative. In a PPLN, the ferroelectric domains are periodically inverted thus there is a periodic nonlinear coefficient distribution.[13] The new frequency components generated from quadratic nonlinearity thus have opposite initial phases (i.e., π phase shift) in positive and negative domains. As long as the light propagation induced phase difference is also π when the domain thickness is well designed, the new frequency components in all domains could interfere constructively resulting in a dramatic efficiency enhancement. This is a simplified picture of QPM, meaning the microstructure may improve the nonlinear effects greatly. As a consequence, it is very interesting and attractive to explore nonlinear SPP devices based on structured QPM materials.

In this paper, we study the nonlinear optical characteristics of SPP at the metal-PPLN interface. Normally the QPM is a photonics principle while we combine such a topic with the excitation of SPP that is a plasmonics principle. A hybrid photonic/plasmonic concept is thus proposed. The coupling equations are deduced to describe the general three SPP-wave interactions, where the SPP attenuation and unique mode distribution play important roles on the power evolution of all frequency components. The QPM condition thus cannot be satisfied ideally. As an example, the second-harmonic generation (SHG) of SPP at the Ag-PPLN interface is investigated. The local-field enhancement of SPP could greatly help the SHG in a very short propagation range. However, the high SPP attenuation is still a barrier to high efficient frequency doubling. A long-range SPP (LRSPP) approach is further proposed, which shows two orders of magnitude efficiency improvement.

II. MODEL AND THEORETICAL SIMULATION

To study a typical QPM three-wave nonlinear interaction, such as SHG, sum-frequency generation (SFG), and difference-frequency generation (DFG), coupling mode theory is normally used.[15] However, although SPP could be viewed as a special guiding wave mode, it has a complex wave vector and very confining field distribution that is quite different from ordinary dielectric waveguide modes. Therefore, the SPP loss and mode features should be taken into account in deducing related coupling wave equations from the Maxwell's equations,

$$\nabla \times E = -\mu \frac{\partial H}{\partial t}$$

$$\nabla \times H = \varepsilon \frac{\partial E}{\partial t} + \chi^{(2)} EE, \tag{1}$$

where E is the electric field, H is magnetic field; μ and ε are the permeability and dielectric constant, respectively. We assume the light propagate along the x axis and treat the nonlinear term $\chi^{(2)}EE$ as a perturbation. Without loss of generality, the field distributions of frequency ω are written as $H_n^{(\omega)}(y,z)$, $E_n^{(\omega)}(y,z)$ at the zero-order approximation for the nth mode with the propagation wave vector of $k_n^{(\omega)}$. Although the SPP is normally a single mode, a general case with multimode are considered, so that the nonlinear interaction between SPP and waveguide modes also could be studied. Follow the standard coupling mode theory in integrated optics,[16]

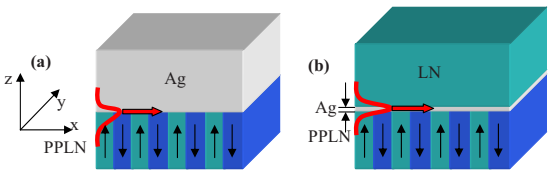

FIG. 1. (Color online) Schematic of the nonlinear frequency conversion of (a) the SPP at Ag-PPLN boundary and (b) the LRSPP propagating in a sandwiched structure of LN-Ag-PPLN.

amplitudes of the electric field and magnetic field could be obtained after the nonlinear perturbation is considered,

$$E = \sum_{n,m} a_n^{(\omega_m)}(x) E_n^{(\omega_m)}(y,z) e^{i(k_n^{(\omega_m)} x - \omega_m t)}$$

$$H = \sum_{n,m} a_n^{(\omega_m)}(x) H_n^{(\omega_m)}(y,z) e^{i(k_n^{(\omega_m)} x - \omega_m t)}, \tag{2}$$

where the amplitude $a_n^{(\omega_m)}$ for the nth mode of frequency ω_{m} obey the following coupling wave equations:

$$\sum_n \left\{ e^{i(\beta_n^{(\omega_q)} - \beta_p^{(\omega_q)^*})x} \int\int [E_{t,n}^{(\omega_q)} H_{t,p}^{(\omega_q)^*} + E_{t,p}^{(\omega_q)^*} H_{t,n}^{(\omega_q)}] dy dz \right\} \times \frac{d}{dx} a_n^{(\omega_q)}(x)$$

$$= \sum_{j,k,l,m,n,c=1,[q/2]} i\omega_q F_{q,c} a_n^{(\omega_c)} a_m^{(\omega_{q-c})} e^{i(\beta_n^{(\omega_c)} + \beta_m^{(\omega_{q-c})} - \beta_p^{(\omega_q)^*})x} \times \int\int E_{j,p}^{(\omega_q)^*} \varepsilon_0 d_{jkl}(y,z,x) E_{k,n}^{(\omega_c)} E_{l,m}^{(\omega_{q-c})} dy dz$$

$$+ \sum_{j,k,l,m,n,c=q+1,\infty} i\omega_q a_n^{(\omega_c)} a_m^{(\omega_{c-q})^*} e^{i(\beta_n^{(\omega_c)} - \beta_m^{(\omega_{c-q})^*} - \beta_p^{(\omega_q)^*})x} \times \int\int E_{j,p}^{(\omega_q)^*} \varepsilon_0 d_{jkl}(y,z,x) E_{k,n}^{(\omega_c)} E_{l,m}^{(\omega_{c-q})^*} dy dz. \tag{3}$$

$F_{q,c} = \{ \begin{smallmatrix} 1 & q \neq 2c \\ \frac{1}{2} & q = 2c \end{smallmatrix}$, where subscripts m, n, and p are the mode numbers; q and c represents different frequencies, j, k, and l represents x, y, and z directions, respectively. t means the field is perpendicular to the propagation direction. In comparison with traditional planar wave's coupled wave equations,[15] Eq. (3) has two differences. First, the coupling coefficients are determined by the overlapping of the involved modes; second, the wave vectors may have imaginary parts that affect the QPM results as well.

Figure 1(a) shows the schematic of a SPP SHG. A metal film is deposited on a PPLN. Because silver has lower light attenuation in 1550 nm telecom window and its second-harmonic wavelength, it is used in our study instead of other metals such as gold. From the figure, an SPP at the Ag-PPLN boundary could be excited, either through attenuated total reflection or grating assistance. Because the PPLN is a second-order nonlinear medium, frequency conversion of the SPP wave thus could be expected. Here we only study a simple case, the SHG of SPP at the Ag-PPLN interface. The frequency conversion is only between the SPP fundamental wave (FW) and SPP SH wave so that only one mode should be considered for a frequency component. Because the SPP frequency doubling caused by surface roughness[17,18] is very weak, it is not considered in our work. In addition, as the nonlinear coefficient d_{33} of LN is the largest one, SHG caused by other nonlinear coefficients, such as d_{31} and d_{22} are neglected. The main effective electric fields of the involved SPP are along Z axis. Meanwhile, the light power of the SPP mode at the entrance port could be normalized, i.e., $\frac{1}{4}\int [E_{z,\mathrm{SPP}}^{(\omega_q)} \times H_{y,\mathrm{SPP}}^{(\omega_q)^*} + E_{z,\mathrm{SPP}}^{(\omega_q)^*} \times H_{y,\mathrm{SPP}}^{(\omega_q)}] dz = 1$. At last, the simplified coupling equations for the SPP SHG over PPLN are obtained as,

$$\frac{d}{dx} a_{\mathrm{SPP}}^{(\omega)}(x) = i\frac{\omega}{4} a_{\mathrm{SPP}}^{(2\omega)} a_{\mathrm{SPP}}^{(\omega)^*} e^{i(\beta_{\mathrm{SPP}}^{(2\omega)} - \beta_{\mathrm{SPP}}^{(\omega)^*} - \beta_{\mathrm{SPP}}^{(\omega)})x} \varepsilon_0 \int E_{z,\mathrm{SPP}}^{(2\omega)} \times (E_{z,\mathrm{SPP}}^{(\omega)^*})^2 d_{33}(x,z) dz$$

$$\frac{d}{dx} a_{\mathrm{SPP}}^{(2\omega)}(x) = i\frac{\omega}{4} a_{\mathrm{SPP}}^{(\omega)} a_{\mathrm{SPP}}^{(\omega)} e^{i(2\beta_{\mathrm{SPP}}^{(\omega)} - \beta_{\mathrm{SPP}}^{(2\omega)})x} \varepsilon_0 \times \int E_{z,\mathrm{SPP}}^{(2\omega)^*} (E_{z,\mathrm{SPP}}^{(\omega)})^2 d_{33}(x,z) dz. \tag{4}$$

Being different from traditional QPM coupling waves, the wave-vector mismatching for FWs and SHs are different, which are $\Delta\beta_1 = \beta_{\mathrm{SPP}}^{(2\omega)} - \beta_{\mathrm{SPP}}^{(\omega)^*} - \beta_{\mathrm{SPP}}^{(\omega)}$ and $\Delta\beta_2 = 2\beta_{\mathrm{SPP}}^{(\omega)} - \beta_{\mathrm{SPP}}^{(2\omega)}$, respectively. When there is no imaginary parts of the involved wave vectors, the FW and SH have the same wave-vector mismatching, and degenerate to the case of traditional SHG. In a PPLN, $d_{33}(x,z)$ is a periodic function of x whose Fourier expansion gives a term $e^{-iG_m x}$. Here Λ is the period and $G_m = m2\pi/\Lambda$ is the reciprocal vector. As long as $\Delta\beta_{1,2} = G_m$, the FW and SH could exchange their power efficiently, which is the QPM condition. However, the wave-vector differences $\Delta\beta_{1,2}$ may have imaginary part but G_{m} is a real number that cannot totally compensate $\Delta\beta_1$ or $\Delta\beta_2$. There is no perfect QPM state for SPP involved frequency conversion while just a best-achievable matching range. We rewrite a "QPM" condition with $G_m = |\mathrm{real}(\Delta\beta_1)| = |\mathrm{real}(\Delta\beta_2)|$, which is an approximate condition used instead. In this case, the corresponding PPLN period could be determined. In another word, the frequency conversion of SPP is still feasible with the help of PPLN at such a "best achievable" imperfect QPM condition.

According to Eq. (4), amplitude evolutions of FW and SH could be calculated for SPP over a PPLN or a single domain LN. Assume the incident FW SPPs intensity is 10 MW/cm (averaged value along the y direction). The incident SPP has the frequency of 193.4 THz, corresponding to a light wavelength of 1550 nm in vacuum. The corresponding effective indices of the FW and SH are $2.19+0.0042i$ and $2.46+0.023i$, respectively. A PPLN with the period of 2.89 μm is thus utilized to match the QPM condition.

Figure 2 shows the FW intensity and SHG efficiency at different sample positions. The FW intensity drops quickly due to the high SPP attenuation. As for the SH, although there is higher intrinsic attenuation, the SH intensity ramps up quickly due to the fed energy from FW through frequency

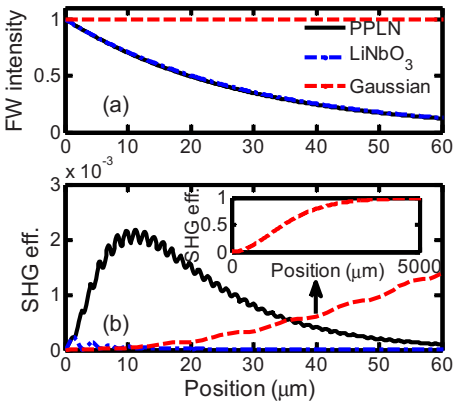

FIG. 2. (Color online) The (a) FW intensity and (b) SHG efficiency at different sample positions, where the solid and dashed-dotted curves correspond to SPP over a PPLN and a single domain $LiNbO_3$, respectively. The dashed curve corresponds to a focused Gaussian beam frequency doubling.

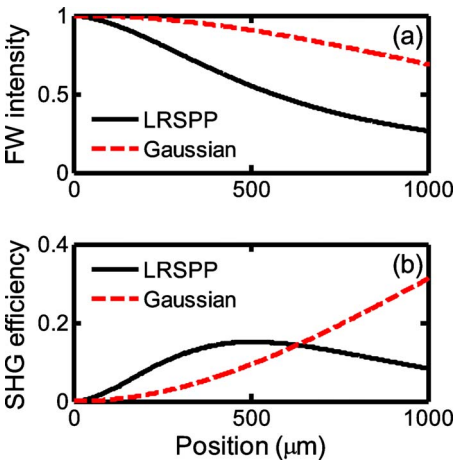

FIG. 3. (Color online) The simulated (a) FW intensity and (b) SHG efficiency at different sample positions. The solid and dashed curves correspond to the LRSPP and focused Gaussian beam, respectively.

doubling. Being different from normal SHG, the SPP SH does not increase smoothly while exhibits a fluctuated trend. There are two local maxima in a PPLN period; one for the positive domain and another one for the negative domain. This is because of the competition between SHG and the high SH attenuation. When the generated SH power flow is balanced by its intrinsic attenuation, a peak or valley comes out. The position where SH drops fastest is at the domain boundary because the locally generated SH is zero. The position with largest ramping slope is at the middle of a domain, where the fed new SH has the largest power flow. When a SPP FW just enters the PPLN-Ag interface, the FW contains the highest intensity so the SH increases quickly. However, when the FW is attenuated after propagating a distance, the locally generated SH also becomes weaker. When the total new SH in a period is exhausted by its attenuation, the efficiency slope reaches its peak value. From Fig. 2, the effective distance for highest SPP SHG is only ~11.2 μm. However, if a single domain LN is used to replace the PPLN, the peak intensity is an order of magnitude lower as shown in the figure, which means the QPM really greatly improves SPP SHG.

The traditional QPM SHG is normally performed in bulk PPLN crystals while the SPP is an attenuated and well-confined spatial mode. Different mode sizes and propagation constants may result in different QPM behaviors. To compare these two extreme cases, we also studied the SHG of a Gaussian distributed bulk FW in a PPLN. The half beam-width along z axis is set at 16.9 μm,[19] which is achievable though focusing a beam into a PPLN. Assume the averaged incident FW intensity along y direction is still 10 MW/cm so that the results could be compared with SPP SHG. For the bulk wave, the FWs and SHs refractive indices are 2.21 and 2.26, which are far different from the case of SPP SHG. The bulk wave shows much weaker dispersion than SPP, thus the required PPLN period increases remarkably to 18.93 μm. From Fig. 2, the SPP SHG has a much higher efficiency than that of a Gaussian FW beam. The high-field concentration of SPP really helps SHG. However, the SPP SHG, saturates and decays quickly due to the lossy FW and SH SPPs. The Gaussian input beam eventually gives rise to higher and higher efficiency because of the negligible loss in PPLN. It reaches ~100% efficiency for a 4.7-mm-long PPLN crystal as shown in Fig. 2(b).

From the above simulation results, the key factor that limits the overall SHG efficiency is the high metal loss of SPP. From our calculation, the FW drops to 1/10 after 67 μm propagation while the SH is even more lossy. 1/10 intensity is left only after 6.2 μm traveling. Although the field enhancement of SPP is very favorable for nonlinear effects, the FW and SH absorptions make a long distance SPP frequency conversion difficult. It may only used in miniature plasmonic circuits.

To improve the long-distance SPP nonlinear effects, the LRSPP might be an effective way. It keeps the features of SPP while has much lower attenuation.[20] On the other hand, for SPP, as shown in Fig. 1(a), if the silver layer is exposed to open air, there are really possible issues of sulfidization or oxidation especially at a high temperature. In this case, it is better to cover the silver layer with some coatings to keep the long-term functionality. However, for LRSPP, the thin metal film is normally sandwiched in two dielectric layers. It does not open in the environmental circumstance that is an advantage to avoid the future degradation.

The proposal of LRSPP SHG is shown in Fig. 1(b). A 10 nm Ag film is deposit on a PPLN. Then another top LN layer is coated above the Ag film for index matching. We assume the top LN is a single ferroelectric domain. This could be achieved by *in situ* field-assisted pulsed laser deposition.[21] The mode distributions and wave vectors of LRSPPs could be computed according to Ref. 20.

Figure 3 shows the simulation results of LRSPP SHG with the same averaged input FW intensity. The Gaussian beam SHG curve is also displayed with dashed line in the figure for comparison. The maximum LRSPP SHG efficiency has been improved dramatically, reaching a peak at 15.2%, even higher than that of the bulk Gaussian beam at this position. The effective length at the peak efficiency is 511 μm. The main reason is the low intrinsic loss of LRSPP.

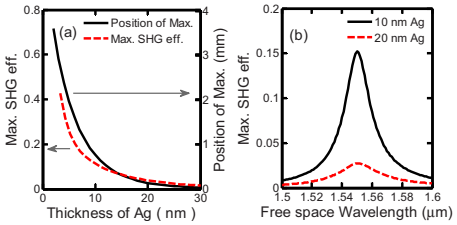

FIG. 4. (Color online) (a) The peak SHG efficiencies and corresponding sample length as a function of the Ag film thicknesses. (b) The efficiency versus free-space FW light wavelength for a 10-nm- and a 20-nm-thick Ag films, respectively.

The position that FW drops to 1/10 intensity is 14.2 mm. The SH also could travel 438 μm with 1/10 intensity left. Both the FW and SH have significantly improved loss so that the peak SHG efficiency is boosted. However, the SPP SHG reaches 0.21% at 11.23 μm position but the efficiency of LRSPP SHG is only 0.05% at the same position. This is because the LRSPP has more dielectric properties while less metallic features than normal SPP. The concentration of the local electric field is much weaker and the mode has broader distribution. The FW and SH mode overlapping and thus the coupling coefficient is reduced. In addition, the top LN layer is just a single domain, it has no contribution to QPM SHG. However, we may also assume a PPLN top layer. A scanning probe technique could be used to induce periodically domain inversion for top PPLN film fabrication.[22] In this case, doubled SHG efficiency could be predicted. However, even there is just a single domain top layer, the SHG efficiency already has been greatly increased due to the lower FW and SH loss.

To further study the QPM frequency doubling of a LRSPP, two important factors should be considered: the metal film thickness and the bandwidth of FW. Because, for the first factor, the properties of LRSPP are sensitively affected by the metal film thickness in general;[20] in addition, the acceptance bandwidth is very necessary in selecting a suitable FW light source to achieve a high SHG efficiency.

First, the peak SHG efficiencies with different metal film thicknesses are calculated. Figure 4(a) shows the results. The corresponding position of maximum is also displayed. The efficiency drops exponentially with an increasing metal thickness. The LRSPP of 10 nm Ag film has a 5.6 times SHG efficiency than that of a 20 nm Ag film. The phenomenon is quite understandable. The thinner Ag film gives rise to wider light field distribution penetrating into the low loss dielectric. For example, the 20 nm Ag film corresponds to a 460 nm full width at half maximum (FWHM) of the SHs magnetic field amplitude but a 10 nm film results in a 710 nm FWHM. If the film thinness is even thinner, the efficiency goes higher and higher, closing to the case of bulk PPLN frequency doubling.

The efficiency as a function of FW light wavelength in vacuum is shown in Fig. 4(b). Two cases with 10 nm and 20 nm Ag films are displayed. From the figure, the wavelength bandwidths for 10 nm and 20 nm Ag films are 22 nm and 36 nm, respectively, which are close to the linewidths of commercial picosecond-to-femtosecond ultrashort lasers. However, thicker Ag film gives rise to wider bandwidth at the optimized sample length. If the metal film is thick enough, LRSPP gradually changes to SPP, a widest FW bandwidth of 176 nm could be obtained. In this case, a femtosecond FW could be used. From the simulation results, there is a tradeoff between wider bandwidth and higher LRSPP SHG efficiency with thinner Ag thickness. To overcome this difficulty, an aperiodic domain structure rather than PPLN may be used so that the bandwidth could be intentionally designed to match the light source.

Furthermore, more information could be revealed in Fig. 4(b). For example, the peak efficiencies are just at 1550 nm, which is the designed center wavelength. Because the PPLNs period is determined according to the best-achievable QPM condition, it means this approximate condition still may assure the best possible energy transfer between the interacted modes. So even for other lossy nonlinear optical system, as long as the wave vector could be written as a complex number with both real and imaginary parts, the similar lossy coupling wave equations such as Eq. (4) could be deduced. Because all our results are based on the coupling wave equations, we believe the best-achievable QPM condition could be applied in other systems beyond plasmonics, for example, PPLN with some absorptive dopants.

III. DISCUSSIONS

From our simulation and analysis above, the reciprocal vector of PPLN could be used to compensate the phase mismatching between SPP FW and SPP SH so that efficient SPP SHG could be achieved. Although the SHG only has a $\sim$11 μm effective sample length, the high-field concentration of SPP already shows benefits in SHG. Actually it might already be acceptable for some plasmonic applications because people are pursuing nanoscale photonic circuits based on SPP. As for the possible SPP absorption induced thermal effect in future practical applications, it could be compensated by some cooling methods to make the device more stable.

In addition to our approach, Liu *et al.* also have reported the enhancement of SPP SHG on periodic subwavelength structured metal film.[17] However, metal is intrinsically a centrosymmetric medium, no strong SHG process can occur even if the surface structure may greatly improve its efficiency. Quadratic nonlinear crystals are still the most practical materials for active plasmonic applications. Davoyan *et al.* recently proposed a phase-matching approach for a $LiNbO_3$ waveguide sandwiched between two silver plates.[23] 6×10^{-3}% SHG efficiency was predicted that is a very exciting result. However, the phase matching is realized between the symmetric and lossy antisymmetric modes. A part of the FW and SH fields have no overlapping that is a barrier for the efficiency improvement. It is also difficult to apply this approach to other nonlinear crystals because of the complicated and strict mode coupling. In addition, the waveguide's slot width should be well designed for phase matching which also limits its applications. On the contrary, QPM is a very efficient way for SHG at any waveguide profile and any working temperature over the material's whole transparency range.

In comparison with the previous reported SPP SHG,[17,23] the QPM SPP and LRSPP SHGs have some great advantages. For example, high efficiency, wide, and adjustable bandwidth and easy implementation in various materials. In addition to SPP SHG, other nonlinear plasmonic parametric processes such as SFG, DFG, and optical parametric amplification (OPA) also could be realized based on PPLN. The corresponding coupling wave equations still could be deduced from Eq. (1). As SFG and DFG in PPLN are proven tools for telecomm logic computation and light switching,[8] we would also expect exciting new ways to manipulate SPPs though quasiphase matching. The QPM OPA even could be used to supply high intensity SPP source or "lossless" SPP for various applications. Actually the pumping source does not need to travel along the signal SPP. A noncollinear QPM approach[12] could be used to greatly suppress the pumping light attenuations. For an OPA at the degenerated wavelength, the generated signal and idler SPPs are identical and possibly "entangled." Because the photon entanglement is a fundamental concept in quantum optics, its counterpart in plasmonics also deserves further investigation. There should be many novel nonlinear plasmonic applications based on QPM in structured metal/dielectric materials.

IV. CONCLUSIONS

In summary, we proposed a QPM nonlinear frequency conversion approach for SPPs. The related coupling wave equations are derived from Maxwell equations. The reciprocal vector of a periodic nonlinear medium is able to compensate the phase mismatching between interacted SPP waves for frequency conversion but an ideal QPM condition is hard to satisfy. The imaginary part of SPPs wave vector and imperfect FW and SH mode overlapping affect the results severely. The imaginary wave vector results imperfect QPM and light absorption so that the SHG may saturate and decay in a thick sample. The partial FW and SH mode overlapping further reduces the frequency conversion efficiency. An Ag film over PPLN is selected for theoretical investigation. The excited SPP wave has higher field concentration than a typical Gaussian beam. The SPP thus shows a much stronger SHG in a short traveling distance. Although the severe attenuation of SPPs limits the highest efficiency, a LRSPP approach was proposed to overcome it. Applications of the SPP frequency conversion were discussed as well.

ACKNOWLEDGMENTS

This work is supported by National 973/quantum manipulation program under Contracts No. 2010CB327803 and No. 2006CB921805, NSFC under Programs No. 60977039 and No. 10874080. The authors also acknowledge the support from New Century Excellent Talents program and Changjiang scholars program. Z. Y. Yu acknowledges the support from the Scientific Research Foundation of Graduate School of Nanjing University under Contract No. 2009CL01.

*Corresponding author.
†feixu@nju.edu.cn
‡yqlu@nju.edu.cn

[1] C. P. Huang, X. G. Yin, Q. J. Wang, H. Huang, and Y. Y. Zhu, Phys. Rev. Lett. **104**, 016402 (2010).
[2] R. F. Oulton, V. J. Sorger, T. Zentgraf, R. Ma, C. Gladden, L. Dai, G. Bartal, and X. Zhang, Nature (London) **461**, 629 (2009).
[3] A. Hohenau, J. R. Krenn, A. L. Stepanov, A. Drezet, H. Ditlbacher, B. Steinberger, A. Leitner, and F. R. Aussenegg, Opt. Lett. **30**, 893 (2005).
[4] R. Gordon, Phys. Rev. B **73**, 153405 (2006).
[5] S. I. Bozhevolnyi, V. S. Volkov1, E. Devaux, J. Laluet, and T. W. Ebbesen, Nature (London) **440**, 508 (2006).
[6] K. A. Tetz, R. Rokitski, M. Nezhad, and Y. Fainman, Appl. Phys. Lett. **86**, 111110 (2005).
[7] L. Feng, M.-H. Lu, V. Lomakin, and Y. Fainman, Appl. Phys. Lett. **93**, 231105 (2008).
[8] Y. L. Lee, B.-A. Yu, T. J. Eom, W. Shin, C. Jung, Y.-C. Noh, J. Lee, and D.-K. Ko, Opt. Express **14**, 2776 (2006).
[9] C. J. Min, P. Wang, C. Chen, Y. Deng, Y. Lu, H. Ming, and T. Ning, Opt. Lett. **33**, 869 (2008).
[10] X. R. Gu, K. Huang, Y. Li, H. F. Pan, E. Wu, and H. P. Zeng, Appl. Phys. Lett. **96**, 131111 (2010).
[11] H. Kamada, M. Asobe, T. Honjo, H. Takesue, Y. Nishida, O. Tadanaga, and H. Miyazawa, Opt. Lett. **33**, 639 (2008).
[12] V. Berger, Phys. Rev. Lett. **81**, 4136 (1998).
[13] Y. Q. Lu, Y. Y. Zhu, Y. F. Chen, S. N. Zhu, N. B. Ming, and Y. J. Feng, Science **284**, 1822 (1999).
[14] K. Gallo, G. Assanto, K. R. Parameswaran, and M. M. Fejer, Appl. Phys. Lett. **79**, 314 (2001).
[15] M. M. Fejer, G. A. Magel, D. H. Jundt, and R. L. Byer, IEEE J. Quantum Electron. **28**, 2631 (1992).
[16] G. Lifante, *Integrated Photonics: Fundamentals* (Wiley, England, 2003), Chap. 4, p. 98.
[17] K. Liu, L. Zhan, Z. Y. Fan, M. Y. Quan, S. Y. Luo, and Y. X. Xia, Opt. Commun. **276**, 8 (2007).
[18] J. C. Quail, J. G. Rako, H. J. Simon, and R. T. Deck, Phys. Rev. Lett. **50**, 1987 (1983).
[19] A. Jechow, D. Skoczowsky, and R. Menzel, Opt. Express **15**, 6976 (2007).
[20] P. Berini, Adv. Opt. Photon. **1**, 484 (2009).
[21] W. S. Hu, Z. G. Liu, Y.-Q. Lu, S. N. Zhu, and D. Feng, Opt. Lett. **21**, 946 (1996).
[22] Y. Kan, X. M. Lu, X. M. Wu, and J. S. Zhu, Appl. Phys. Lett. **89**, 262907 (2006).
[23] A. R. Davoyan, I. V. Shadrivov, and Y. S. Kivshar, Opt. Express **17**, 20063 (2009).